



UNIVERSITY OF LEEDS

This is a repository copy of *Original Sedimentary Pattern of an Inverted Basin: A Case Study from the Bozhong Depression, Offshore Bohai Bay Basin*.

White Rose Research Online URL for this paper:
<http://eprints.whiterose.ac.uk/112425/>

Version: Accepted Version

Article:

Zhao, J, Liu, C, Huang, L et al. (4 more authors) (2016) Original Sedimentary Pattern of an Inverted Basin: A Case Study from the Bozhong Depression, Offshore Bohai Bay Basin. *Acta Geologica Sinica - English Edition*, 90 (6). pp. 2163-2181. ISSN 1755-6724

<https://doi.org/10.1111/1755-6724.13029>

(c) 2016, Wiley. This is an author produced version of a paper published in *Acta Geologica Sinica - English Edition*. Uploaded in accordance with the publisher's self-archiving policy.

Reuse

Items deposited in White Rose Research Online are protected by copyright, with all rights reserved unless indicated otherwise. They may be downloaded and/or printed for private study, or other acts as permitted by national copyright laws. The publisher or other rights holders may allow further reproduction and re-use of the full text version. This is indicated by the licence information on the White Rose Research Online record for the item.

Takedown

If you consider content in White Rose Research Online to be in breach of UK law, please notify us by emailing eprints@whiterose.ac.uk including the URL of the record and the reason for the withdrawal request.



eprints@whiterose.ac.uk
<https://eprints.whiterose.ac.uk/>

Original sedimentary extent of an inverted basin: a case study from the Bozhong Depression, offshore Bohai Bay Basin

ZHAO Junfeng^{1*}, LIU Chiyang¹, HUANG Lei¹, HAN Shaojia², LIU Peng³, HU Junhao⁴

1 State Key Laboratory of Continental Dynamics/ Department of Geology, Northwest University, Xi'an 710069, China

2 Gansu Coal Geological Research Institute, Lanzhou 730000, China

3 Key Laboratory of Petroleum Resources Research, Institute of Geology and Geophysics, Chinese Academy of Sciences, Lanzhou 730000, China

4 Institute of Geochemistry, Chinese Academy of Sciences, Guiyang 550002, China

Abstract: The third member of Shahejie Formation (Sha-3 Member; Eocene) in the Bozhong Depression, offshore Bohai Bay Basin was subject to multiple post-depositional modifications. Analysis of this succession demonstrates that the present structural framework of the Bozhong Depression, which is characterized by sags alternating with rises, does not reflect its original sedimentary pattern. Issues related to post-depositional modification, which include changes to the original sedimentary extent and the depositional geodynamic setting of the Sha-3 Member, have not been discussed in detail previously. In this study, the characteristics of the post-depositional modification and original sedimentary extent of the Bozhong Depression are investigated through analysis of seismic and well-log data, in combination with fission-track analysis. Results demonstrate that the Shijiutuo Rise, a major structural feature of the current basin, did not exist at the time of accumulation of the Sha-3 Member, such that the Qinnan Sag was largely connected to the Bozhong Sag to form a single contiguous area of deposition within the basin. By contrast, the Shaleitian and Chengbei rises, located in the western part of the Bozhong Depression, were already developed at the time of accumulation of Eocene Sha-3 Member; these features were manifested as syn-depositional tilted fault blocks, the uplifted footwall blocks of which provided sediments for the neighboring Shanan and Chengbei sags. The western part of the Bonan Low Rise, located in the southern part of the Bozhong Depression, did not experience uplift during the phase of accumulation of the Eocene Sha-3 Member. The Huanghekou Sag was connected with the Bozhong Sag in the central and western part of the Bozhong depression. The original sedimentary boundary of the South Miaoxi Sag possibly extended eastward about 10 km to connect with the Bozhong Sag at its northern margin. The present-day Bodong Low Rise, which is bounded by the Tan-Lu Fault Zone, also formed after accumulation of the Eocene Sha-3 Member. By combining all these observations, it can be concluded that the Bozhong Depression formed a connected large-scale sub-basin during accumulation of the Eocene Sha-3 Member: several neighboring sags that are now separated by rises, including the Qinnan, Shanan, Chengbei, Huanghekou, Miaoxi and Bodong sags, formed a single contiguous depositional area during the Eocene. Marked differences in basin extent and framework between the sedimentary stage and present-day stage provide a valuable case study for gaining an improved understanding the history of basin inversion and its impact on related hydrocarbon-system evolution.

Keywords: Eocene; Shahejie Formation; basin inversion; Bozhong depression; Bohai Bay Basin

1 Introduction

Basin inversion is a term used to indicate the shortening of formerly extensional basins (Marco et al, 2012). The inversion of sedimentary basins has been the focus of considerable research (e.g., James, 1995; Kevin et al, 1995; Ziegler et al, 1995; Turner et al, 2004; Marco et al, 2012) because such behavior has significant

* Corresponding author E-mail: zjf@nwu.edu.cn

48 implications for basin mechanics that influences basin-scale hydrocarbon prospectively. Although previous
49 studies regarding basin inversion have mainly focused on inversion styles and the mechanics of such behavior
50 (e.g., Mike, 1999; Susanne et al, 2009; Jarosinski et al, 2011), relatively few studies have considered and
51 discussed the original sedimentary extent of inverted basins in detail. Basin inversion is widely noted from
52 Cenozoic rifted basins in eastern China. In many cases, such inversion events occurred at or shortly after the
53 transition from the rift to the post-rift stages in these basins (Allen et al, 1997; Song, 1997). By contrast, the
54 recognition of major inversion phenomenon that occurred during the rifting stage has been noted and discussed
55 in detail only relatively recently (Huang et al, 2012a, 2014a).

56 The Bohai Bay Basin originated as a consequence of the destruction of the North China Craton (Li et al.,
57 2012a, 2012b). This basin has been the focus of a large number of research studies in recent years (e.g., Li et al,
58 2013; Zhou et al., 2012; Huang et al, 2012a, 2014a; Han et al, 2014). The Bozhong Depression, located in the
59 offshore Bohai Bay Basin, is one of the most important petroliferous areas in China (Fig.1). Within the
60 sedimentary fill of this depression, exploration data have shown that the third member of Eocene Shahejie
61 Formation (Sha-3 Member) is the primary hydrocarbon source interval in this region. Within the Bozhong
62 Depression hydrocarbons are mostly accumulated in sags and their adjacent rises, and reservoirs exhibit the
63 characteristics of oil and gas accumulation controlled by hydrocarbon-enriched sags (Gong, 1997; Yang and Xu,
64 2004; Deng, 1999; Zhu et al, 2009; Huang et al, 2014b; Fig. 1). Previous studies have revealed that the
65 Bozhong Depression underwent two evolutionary stages in the Cenozoic: a Paleogene rift state and a Neogene
66 post-rift stage (Tab. 1). Within the fill of the Bozhong Depression, seismic and well data reveal the Sha-3
67 Member is absent from the crest regions of several prominent rises and it has been argued previously that these
68 rises were present as geomorphic highlands that were subject to denudation at the time of accumulation of the
69 Sha-3 Member (Zhu et al, 2009; ECOHG, 1990; Zhao et al, 1996; Xu et al, 2008; Qi et al, 2008; Jiang et al,
70 2009; Li et al, 2011; Zhou et al, 2011). Although several tectonic interfaces are recognized from seismic data
71 from the Bozhong Depression, such as Sha-4/Sha-3 (T_6), Sha-3/Sha-2 (T_5) and Guantao/Dongying (T_3)
72 interfaces (ECOHG, 1990; Qi et al, 2008), only recently has the significance of post-depositional reworking
73 events that occurred during the late Eocene and the late Oligocene been highlighted in terms of their
74 significance for understanding the modification of the pre-existing Paleogene basin (Wu et al, 2006; Huang et
75 al, 2012a, 2014a). This modification implies that the present-day pattern of distribution of strata of the Sha-3
76 Member cannot represent the original sedimentary framework. This issue is very important for the assessment
77 of hydrocarbon resources; furthermore, it is also of considerable theoretical significance for developing an
78 improved understanding of the evolutionary and reworking process of lacustrine rifted basins. Indeed, many
79 important research questions relating to such issues remain unanswered: what were the processes of reworking
80 that deposits of the Sha-3 Member experienced, and what was the original sedimentary extent and
81 paleogeographic setting of the basin during Sha-3 period?

82 This study mainly focuses on the above-mentioned issues, and outlines an approach to the reconstruction of
83 the modified basin (cf. James, 1995; Kevin, 1995; Liu and Sun, 1999; Liu and Yang, 2000; Zhao et al, 2010).
84 The aim of this study is to reconstruct the original extent and framework of the Bozhong Depression during the
85 accumulation of the Eocene Sha-3 Member, and to discuss the genetic mechanisms and hydrocarbon
86 implications of the inversion event. This is achieved through investigation of stratigraphic contact relationships,
87 investigation of the type of sedimentary systems, analysis of sediment provenance and reconstruction of the
88 history of uplift of several prominent rises. Specific research objectives of this study are as follows: (1) to
89 reconstruct the original sedimentary extent and framework of the Bozhong Depression in the offshore Bohai
90 Bay Basin; (2) to demonstrate the importance of a basin inversion event that occurred during the rifting stage;
91 (3) to discuss the implications of such inversion for resources assessment of the pre-existing source rock and
92 hydrocarbon exploration. The principal data used in this study are from over 200 interpreted seismic sections,
93 43 wells and fission track analysis (FTA) of 10 samples.

94 **2 Distribution and modification of the Sha-3 Member in the Bozhong Depression**

95 **2.1 Distribution of the Sha-3 Member**

96 The Paleocene Kongdian Formation and Sha-4 Formation accumulated locally and separately in the
97 Bozhong Depression. By contrast, the Sha-3 Member accumulated widely in the offshore Bohai Bay Basin (Tab.
98 1). Based on analysis of seismic and well-log exploration data, the Sha-3 Member was widely distributed in
99 Bozhong, Qinnan, Nanbu, Shan'an, Chengbei, Huanghekou, Miaoxi and Bodong sags. Between these sags, strata

100 of the Sha-3 Member were separated by several rises, notably the Shijiutuo, Chengbei, Bonan, Miaoxi, Bodong
101 rises. Strata of the Sha-3 Member vary in preserved thickness from ~200-600 m in most parts of the Bozhong
102 Depression, but can attain 600-1400 m locally in the Bozhong, Qinnan, Shanan and Huanghekou sags (Fig.12;
103 Xia et al, 2012). Significantly, accumulated deposits of this member are not present over the crests of the rises.
104 Common lithofacies types of the Sha-3 Member include conglomerate, pebbly sandstone, dark green mudstone
105 and oil shale. Due to a complex history of basin subsidence and inversion, the present-day burial depth of Sha-3
106 Member varies between different sags, ranging from 500 to 8000 m below sea level.

107 **2.2 Overview of Tectonic modification of the Sha-3 Member**

108 The basis for the reconstruction of the original sedimentary extent of the Sha-3 Member is the identification
109 of the style and intensity of modification of strata that form the fill of the Bozhong Depression. Numerous
110 seismic profiles demonstrate that the Sha-3 Member experienced various post-depositional inversions in
111 different areas of the Bozhong Depression, and four types of post-depositional tectonic modification are
112 identified (Tab.2).

113 (1) Tilting by compression. Due to regional compression, the Sha-3 Member and its underlying strata
114 became tilted, uplifted and partly eroded, resulting in the development of a widespread unconformity between
115 the strata of the Sha-3 Member and their overlying units.

116 (2) Tilting by strike-slip movement. Mainly due to activity along the Tan-Lu Fault Zone, strata of the Sha-3
117 Member in some parts of the Bozhong Depression experienced intensive transpressional deformation, leading to
118 tilting and partial erosion.

119 (3) Uplifting by block-faulting. In places, strata of the Sha-3 Member were uplifted and partly eroded in
120 response to post-depositional block-faulting within evolving sags.

121 (4) Regional uplift. Strata of the Sha-3 Member were uplifted as a whole in one sag such that strata at the
122 margins of this sag partly eroded.

123 Relationships on the various seismic profiles demonstrate that these major modifications to the basin fill
124 occurred at the end of Eocene shortly after the completion of accumulation of the Sha-3 Member. In addition,
125 regional uplift at the end of Oligocene also played an important role in further modification, leading to additional
126 erosion in the marginal area of sags.

127 **3 Relationship between the Bozhong Sag and its neighboring structural units**

128 Key to the reconstruction of the original sedimentary extent of Sha-3 Member is the identification of the
129 original relationship between the Bozhong Sag and its surrounding structural units. Two questions are addressed:
130 (1) did the presently observed rises exist during accumulation of the Sha-3 Member? (2) did the regions currently
131 represented by separated sags form a contiguous region during the Eocene for accumulation of the Sha-3
132 Member?

133 **3.1 The Northwestern area of the Bozhong Depression**

134 The Qinnan Sag lies to the northwest of the Bozhong Sag. The two sags were separated by the
135 approximately EW-trending Shijiutuo Rise (Fig.1), a tectonic feature that most researchers argue developed
136 prior to the Paleogene (Lai et al,2007; Xu et al, 2008; Jiang et al, 2009; Li et al, 2011).

137 Analysis of NW-SE- and NE-SW-trending seismic profiles (Figs.2①②) indicate that the Sha-3 Member in
138 the southern part of the Qinnan Sag close to the Shijiutuo Rise underwent intense uplift and erosion, resulting in
139 a truncational contact with the overlying Sha-2 Member. Sha-3 strata preserved beneath the truncated contact dip
140 steeply to the north. This observation is especially evident in the region to the west of well Q27-2-1. The amount
141 of eroded strata is deduced from observations of lateral changes in preserved stratal thickness, which indicate
142 that 150-155 m of strata of the Sha-3 Member were eroded from the southern Qinnan Sag to the Shijiutuo Rise.
143 The region of partial erosion of strata of the Sha-3 Member can be traced for 15-20 km to the northwest of
144 Bozhong Sag and link to strata of the Sha-3 Member in the Bozhong Sag. This observation suggests that the west
145 and middle part of the Shijiutuo Rise did not exist during the Eocene accumulation of the Sha-3 Member.
146 However, the area around the Q28-2 structure in the north-eastern part of the Shijiutuo Rise reveals a different
147 situation: here, strata of the Sha-3 Member overlap and pinch-out from the Qinnan and Bozhong sags to the
148 Shijiutuo Rise, indicating the existence of a pre-existing small-scale rise in this region. To the east, there is an
149 EW-trending horst named structural zone 428. The S-N-trending seismic profiles across structural zone 428
150 demonstrate that the Paleogene strata on both sides are truncated by high-angle normal faults, indicating that the

151 sedimentation during Sha-3 stage was not controlled by the EW-trending structural zone 428 (Fig.2③).

152 Five wells penetrate through Sha-3 Member on the south-eastern flank of the Shijiutuo Rise. Well Q34-2-1 at
153 the south-eastern part of the rise reveals 400 m of Sha-3 strata. The lower interval of this succession is
154 characterized by muddy siltstone interbedded with mudstone, whereas the upper interval is characterized by a
155 combination of multiple units of mudstone, oil shale and muddy dolomite. These lithological associations reflect
156 the paleo-environment, which likely occupied a distal position within the basin, far from any clastic sediment
157 entry point, and likely in a deep-water setting. Well B10 at the west of the structural zone 428 reveals 56 m
158 thickness of Sha-3 strata, of which the lower interval is composed mainly of grayish-white and grayish-green
159 mudstone interlayered with calcareous sandstone, dolomitic limestone, whereas its upper interval is composed of
160 grayish-white sandstone, interbedded with 10 layers of sandy conglomerate. The well B13 to the east mainly
161 reveals grayish-white sandstone interbedded with mudstone, and a 3 m-thick pebbly sandstone interlayer. This
162 lithological association indicates a depositional setting that was relatively proximal to the source area. Thus, it
163 can be inferred that an uplift of modest size likely existed close to well B10, an interpretation that is consistent
164 with the stratigraphic configuration indicated by overlaps and pinch-out phenomenon on the aforementioned
165 seismic profiles.

166 Fission-track analysis (FTA) has been used to determine the timing of uplift of the Shijiutuo Rise. Samples
167 were collected from the shallow buried basement on the rise (Tab.3; Fig.3, 4). The fission-track ages of three
168 apatite samples are far younger than the ages of their host formation. This result indicates that the samples
169 experienced full annealing and subsequent cooling. Therefore, they are suitable for analysis of the uplift history.
170 The χ^2 test values of well Q32-6-2 and Q33-1-1 located close to the crest of the rise are zero, with a bimodal age
171 distribution. Age data were processed with the BinomFit software (Brandon, 1996), to derive decomposition
172 apatite ages of 29Ma and 43 Ma for well Q32-6-2, and 27 Ma and 46 Ma for well Q33-1-1 (Fig. 3). These
173 decomposition apatite ages record two cooling or uplift events in the Early Paleogene and Late Eocene-Early
174 Oligocene, respectively. Of these, the earlier event corresponds to the time of post-depositional uplift and
175 modification of the Sha-3 member. With regard to the distribution of fission-track lengths, both samples have a
176 similar number of long and short tracks, with characteristics of wide unimodal distribution of short tracks (Fig.
177 4). From combination with simulation results (Fig. 5) it is evident that the sample stayed longer in the partial
178 annealing zone. Collectively, results from analysis of the data from the two samples suggest that the main body
179 of Shijiutuo Rise acted as a region of sediment accumulation during the Eocene Sha-3 Stage. The central
180 fission-track age derived from well Q27-2-1 at the east of the rise is 42 ± 4 Ma (Tab. 3), which indicates uplift
181 activity early in the episode of accumulation of the Sha-3 member at this location.

182 In summary, the Shijiutuo Rise did not exist during the deposition of Sha-3 Member. The original
183 sedimentary extent of the Qinnan Sag extended southwards and might have been connected with the Bozhong
184 Sag (Fig. 6). Provenance analysis indicates that coarse-grained clastic sediment was mainly supplied from the
185 northern Qinnan Rise. However, additional evidence implies that small-scale uplift, of limited areal extent
186 (probably around 100 km²), might have occurred in north-eastern part of the area now represented by the
187 Shijiutuo Rise during the Eocene Sha-3 Stage, as demonstrated by (1) seismic reflection data that reveal an
188 onlapping contact; (2) multi-layered coarse grained sediments from well B10, and (3) uplift timing constrained
189 by the fission-track ages from well Q27-2-1 (Tab. 3).

190 3.2 The western area of the Bozhong Depression

191 Exploration data show that the Sha-3 Member is continuously traceable between the Bozhong Sag and the
192 Nanbu, Shanan, and Chengbei sags to its west. This implies that the Sha-3 strata in these sags formed a
193 contiguous area of active sedimentation during accumulation of the Sha-3 Member. A key research question to be
194 answered is whether the Shaleitian Rise and the Chengbei Low Rise that are now present between these sags
195 existed during the Sha-3 Stage?

196 3.2.1 The Shaleitian Rise and the Shanan Sag

197 Seismic profiles show that the Shaleitian Rise is cored by basement rocks with a flat relief (Fig.7①).
198 Cenozoic strata on this rise are mainly composed of the Oligocene Dongying Formation and
199 Neogene-Quaternary strata. The basement rocks comprise Mesozoic-Palaeozoic-Archean sedimentary,
200 metamorphic and magmatic rocks (Fig. 13(a)). Analysis of SN-trending seismic profiles reveal that strata of the
201 Sha-3 Member close to the southern margin of the Nanbu Sag exhibit an onlapping contact with flat strata and no
202 faulting is evident (Fig.7①). At the northern margin of the Shanan Sag, seismic profiles show thickening strata

203 controlled by syn-depositional listric normal faults.

204 The SN-trending profiles across the Shanan Sag reveal that the seismic facies of Sha-3 Member near the
205 Shaleitian Rise are characterized by chaotic reflectors of varied amplitude, which define a wedge-shape body,
206 which is most obviously interpreted as a fan-delta sedimentary system (Fig.7①). By contrast, in the central part
207 of the Shanan Sag, the seismic data are characterized by parallel, continuous and medium-low frequency
208 reflectors, which are most obviously interpreted as moderate- to deepwater lacustrine facies. To the south of this
209 region, close to the Chengbei Low Rise, the seismic data reveal an onlapping contact of wavy, weak continuous
210 and medium amplitude reflectors, which is indicative of shoreline or shallow-water lacustrine or braided
211 delta-plain facies. These observations indicate that the Shanan Sag, from north to south, has an architectural
212 configuration that is typical of a half-graben, characterized by a syn-depositional faulted contact at the north
213 margin. Well data demonstrate that the central Shanan Sag is mainly filled by grayish-green and grayish-black
214 mudstone. Close to the margins of this sag, the proportion of sandstone increases. Particularly, in wells C8-4-1
215 and C8-5-1 at the southern margin of the Shaleitian Rise, the Sha-3 Member is mainly composed of very-thick
216 beds of pebbly sandstone, indicating a location close to the sediment source (Fig.8).

217 Based on the above analysis, the Shaleitian Rise was at least partly developed during the accumulation of the
218 Sha-3 Member. As a syn-depositional tilted fault block, the Shaleitian Rise served as the local sediment
219 provenance for both the southern Shanan Sag and the northern Nanbu Sag, which were themselves interlinked
220 with the Bozhong Sag to their east. This suggestion has been confirmed by fission-track dating results from this
221 region (Tab.3; Fig. 3,4). Aside from the sample from well C4-1-1, which has a lower reliability due to a paucity
222 of particles suitable for analysis, other samples from three wells contain sufficient evolutionary information to
223 constrain the uplift activity during and after the deposition of the Sha-3 Member (Tab. 3; Fig.3).

224 3.2.2 The Chengbei Low Rise and the Chengbei Sag

225 The basement of the Chengbei Low Rise is composed of a series of Paleozoic strata that take the form of a
226 simple, north-tipping monocline (Fig. 13(a)). The Chengbei Sag to the south of the Chengbei Low Rise has a
227 similar half-graben structural configuration to the Shanan Sag; the Sha-3 Member in the Chengbei Sag displays a
228 faulted contact to the north and an overlapping contact to the south (Fig.7②). A thick succession of strata of the
229 Sha-3 Member was controlled by syn-depositional faulting at the northern margin of the Chengbei Sag. By
230 contrast, to the south of the Chengbei sag, the strata underlying the Sha-3 Member near the Chengzikou Uplift
231 change from Sha-4 Member to basement rocks via an onlapping contact relationship with underlying strata.
232 Additionally, low-angle angular truncations can be observed on the top. These observations indicate that slight
233 uplift and erosion occurred in the marginal area of the Chengbei Sag after the accumulation of the Sha-3 Member.
234 The seismic facies in the northern part of the Chengbei sag are characterized by chaotic and wedge-shape
235 reflections, likely indicating sediment accumulation proximal provenance. The seismic reflections in the central
236 part of the sag are characterized by continuous, parallel and medium-low frequency reflections, indicating
237 moderate- to deep-water lake sedimentary facies (Fig.7②). In the area around the Chengzikou Rise, the seismic
238 reflections are characterized by continuous, high-to-medium frequency reflectors with varied amplitudes that are
239 typical of shallow lake sedimentary facies. Additionally, an imbricate, progradational wedge-shape sediment
240 body defined by reflections is most obviously interpreted as a fan-delta front sedimentary facies. All these
241 observations suggest that the Chengbei Low Rise developed as a syn-depositional tilted block during
242 accumulation of the Sha-3 Member, the uplifted footwall of which supplied sediment to the Chengbei Sag and
243 Shanan Sag. In response to continued uplift since the late Eocene, strata of the Sha-3 Member at the southern
244 margin of the Shanan Sag have been partly eroded.

245 3.3 The southern area of the Bozhong Depression

246 The present-day EW-trending Bonan Low Rise is divided into two portions by the Tan-Lu strike-slip fault
247 (Fig.1). The hydrocarbon-enriched Huanghekou Sag is located to the south of this rise. The western part of the
248 Bonan Low Rise has a horst structural configuration, both sides of which are bounded by normal faults. Within
249 this portion of the rise, there are thin preserved accumulations of the Sha-3 Member, which nearly connect to
250 thicker deposits in the Huanghekou and Bozhong sags (Fig.9①②). The boundary faults of the rise extend
251 upward into Neogene and Quaternary successions vertically. These observations indicate that the horst structure
252 was generated by tectonic activities that post-date the Sha-3 stage.

253 Analysis of SN-trending seismic profiles from the eastern part of the Bonan Low Rise indicate that the strata
254 that underlie the Sha-3 Member in the Bozhong Sag thin southwards, and are also present in marginal area of the

255 rise with an onlapping contact (Fig.10①). From the Bozhong Sag towards the Bonan Low Rise, the character of
256 seismic reflections gradually changes from parallel, strong amplitude and highly-continuous to parallel, medium
257 continuous and medium amplitude. Near the Bonan Low Rise, the reflections are chaotic but define a wedge
258 shape progradation body that is most obviously interpreted as fan-delta facies. The same phenomenon can also
259 be identified on the seismic profiles across the Bonan Low Rise and the Huanghekou Sag (Fig.10②). These
260 observations demonstrate that the eastern part of the Bonan Low Rise might have been a pre-existing uplift that
261 provided a local sediment source for the sags at either side during accumulation of the Sha-3 Member; however,
262 it could have been smaller than its present-day configuration.

263 Well data indicate that the grain size of clastic rocks of Sha-3 strata become increasingly fine-grained from
264 north to south, possibly indicating an increasing depth of water and distance from the source of sediment supply
265 from north to south. The mean apatite fission-track age of the samples from the southern margin of the Bonan
266 low rise is 21 ± 2 Ma, indicating that regional tectonic uplift events occurred during the Late Oligocene-Early
267 Miocene (Tab. 3; Fig. 3). The confined track length is characterized by a unimodal distribution, with the lean
268 towards long tracks of the peak value, which indicates a slow cooling process (Fig. 4). This probably resulted
269 from temperature compensations induced by the relatively thick sediment of Dongying Formation and
270 Neogene-Quaternary cover, in that this process can lead to the failure to record the Early Paleogene uplift events
271 by the fission-track data.

272 In summary, the western part of the Bonan Low Rise formed after the deposition of the Sha-3 Member.
273 Whereas, the eastern part of the Bonan Low Rise was already at least partly developed and acted to supply
274 sediment to the adjoining northern and southern sags during the Sha-3 stage. The eastern part of the rise was
275 likely smaller than its present-day configuration. Thus, the Bozhong and Huanghekou sags were interlinked in
276 the middle and western part of the Bonan Low Rise.

277 3.4 The eastern area of the Bozhong Depression

278 3.4.1 The Miaoxi area

279 The Miaoxi region is composed of the southern, northern and eastern sub-sags (Fig.1). Analysis of EW- and
280 NW-SE-trending seismic profiles demonstrates that the Miaoxi sag underwent intensive tectonic uplift in the late
281 Eocene, which resulted in substantial erosion of strata of the Sha-3 Member to east of the sag; this erosion is
282 most conspicuous in the southern sub-sag (Fig.11①). Modification at the eastern and northern sub-sags was
283 relatively weak. Seismic facies and fission-track data reveal that the southern and northern sub-rises were
284 already partly developed during deposition of the Sha-3 Member (Tab. 3; Fig. 3,4). The two sub-rises, as an
285 uplifted fault block, provided sediments for the northern and eastern sub-sags. Restoration of the eroded
286 thickness reveals that the original sedimentary boundary of southern sub-sag extended eastward for 10 km
287 relative to its present extent during deposition of the Sha-3 Member (Han et al, 2014; Huang et al, 2014a). Based
288 on previous systematic analysis (Han et al, 2014), the northern and eastern sub-sags were interlinked with the
289 Bodong Sag, whereas, the southern sub-sag was interlinked with the Huanghekou and Laizhou Bay sags.

290 3.4.2 The Bodong Low Rise and Bodong Sag

291 The Bodong Low Rise intermittently spreads along the Tan-Lu Fault Zone (Fig.1). It is composed of two
292 segments. Well P7-1-1 on the southern Bodong Low Rise reveals that the basement rock is Mesozoic volcanic
293 rock, and the oldest Paleogene strata comprise a 50 m-thick interlayer of mudstone and sandstone of the
294 Kongdian Formation, which is directly overlain by the second member of the Oligocene Dongying Formation.
295 The Shahejie Formation is absent in this well. Well and seismic data indicate that strata of the Sha-3 Member in
296 the Bodong Sag are distributed widely, and have a preserved thickness that varies from 300-1000 m.

297 Analysis of seismic profiles across the Bozhong and Bodong sags demonstrates that the Bodong Low Rise
298 is a faulted anticline bounded by two faults (Fig.11②). Close to the crest of the rise, the Sha-3 Member
299 underwent conspicuous truncation and was cut by faults at the rim of the rise. The Sha-3 member here does not
300 show syn-kinematic characteristics. By contrast, the strata of the Sha-2 and Sha-1 members and the Dongying
301 Formation show a thinning trend from the central sag to the boundary fault, indicating the control of the uplift
302 process exerted by development of the rise. Combined with the stratigraphic sequence revealed by well P7-1-1, it
303 can be inferred that the rise might not have existed during accumulation of the Paleogene Kongdian Formation
304 and Shahejie Formation. the area formed a depocentre together with the sags to its east and west until the end of
305 the Sha-3 Stage; only after this was this region was uplifted and eroded as a result of tectonic inversion. This
306 interpretation is consistent with results from previous studies (Wang et al, 1998; Huang et al, 2012a, 2012b).

307 Therefore, the Bozhong and Bodong sags were likely inter-connected during deposition of the Sha-3 Member.

308 **4 Discussion**

309 **4.1 Original extent and framework during deposition of Sha-3 Member**

310 Based on analysis of seismic and well-log data, post-depositional inversion strongly modified the original
311 sedimentary basin of the Bozhong Depression. During accumulation of Sha-3 Member, many neighboring sags,
312 including the Qinnan, Shan'an, Chengbei, Huanghekou, Miaoxi and Bodong sags, were interlinked with the
313 Bozhong sag, such that the area formed broad, contiguous region of deposition around the current Bozhong sag.
314 Notably, the Shijiutuo Rise acted as an area of deposition during the Eocene Sha-3 Stage, resulting in the
315 connection of the Qinnan and Bozhong sags at that time. The Shaleitian and Chengbei rises were pre-existing
316 uplifts in the Eocene and shed sediments into their adjacent Shan'an and Chengbei sags, respectively. The eastern
317 parts of the Shan'an and Chengbei sags were interlinked with the Bozhong sag. The western part of the Bonan
318 Low Rise was not uplifted during the deposition of the Sha-3 Member. Although the main body of eastern part of
319 the Bonan Low Rise was at least partly developed at this time, it likely was smaller in size than its current extent.
320 Consequently, the central and western parts of the Huanghekou Sag interlinked with the Bozhong Sag, and the
321 central and northern parts of the Miaoxi Sag interlinked with the Bozhong Sag. The present Bodong Low Rise is
322 a later-formed structure constrained by the Tan-Lu Fault Zone. The Bodong Sag formed a part of the large
323 Bozhong Sag during and before the Sha-3 stage (Fig. 12).

324 **4.2 Forming background of the Eocene Bozhong Depression**

325 Analysis undertaken for this study demonstrates that the Nanbu, Shan'an and Chengbei sags to the west of
326 the Bozhong sag were all half-grabens controlled by NWW-trending syn-depositional faults (Fig.13a). The
327 stratigraphic age of the basement rocks in the Shaleitian Rise and the Chengbei Low Rise become older from
328 south to north, indicating that the rises underwent a gradually weakening uplifting and erosion process from
329 south to north; this relationship also records the uplift of fault blocks during sedimentation (Fig.13a). The eastern
330 part of the Bonan Low Rise has a gradually older stratigraphic age of basement from north to south, which also
331 demonstrates similar features of uplift of a fault block during deposition of the Sha-3 Member (Fig.13a). Notably,
332 the southern boundary fault of the Bonan Low Rise is sub-parallel with the faults in the central and western
333 Bozhong regions, and all of them generally trend in a NWW direction. Therefore, ignoring the influence of later
334 modification, subsidence in the western and the southern Bozhong region was controlled by the NWW-trending
335 normal faults, indicating an NNE-SSW-trending extensional stress field during the Eocene Sha-3 stage. However,
336 the rifting feature characterized by normal faulting of boundary faults did not exist in the central Bozhong sag.
337 Instead, the strata of the Sha-3 Member and overlying strata all exhibit characteristics of thickening toward the
338 central part of the Bozhong Sag (Fig.13b). These observations indicate that the central part of the Bozhong Sag
339 was the depocenter of the basin during the Eocene.

340 Combined with previous studies of deep geophysical data (Liu et al,1996; Teng et al,1997; Li, 1997; Zhang,
341 2000 Wang et al,2002; Qi et al,2008), it is here suggested that, aside from the control of the NNE-SSW regional
342 extensional stress field, the subsidence of the Bozhong Sag was probably controlled by deep geological
343 processes during accumulation of the Sha-3 Member. This study of the uplift history of the Bodong Low Rise
344 implies that the Tan-Lu Fault Zone did not reactivate during deposition of the Sha-3 Member, and the same result
345 was also suggested as an outcome of an earlier study of the Liaodong Low Rise (Huang et al, 2012a, 2015).
346 Taking account of the evolutionary history of the entire Bohai Bay Basin, the Sha-3 Member likely accumulated
347 in an overall setting characterized by a regional rift-related subsidence, following initial, localized rift-related
348 subsidence associated with accumulation of the Kongdian Formation and Sha-4 Member. Thus, accumulation of
349 the Sha-3 Member likely reflects both localized faulting and regional tectonics subsidence to form the larger
350 Bozhong Depression.

351 **4.3 Implication for hydrocarbon exploration**

352 This study demonstrates that the Bozhong Depression was much larger during deposition of Sha-3 Member,
353 which serves as the major source rock interval in the offshore Bohai Bay Basin. Consequently, the evaluation of
354 the quantity of hydrocarbon generation in the Bozhong region (especially in the small sags considered herein)
355 should be reconsidered. It is not appropriate to consider the small sags individually. Rather, the depositional
356 extent of the original source rock should be considered in light of findings from this study. Specifically, some
357 residual sags, which are now separated from the original large Bozhong Sag (e.g., Miaoxi and Qinnan sags), may

358 have a greater potential for hydrocarbon generation and accumulation than previous suggested. During recent
359 exploration, the Miaoxi Sag has been proven as a hydrocarbon-enriching sag (Zhu et al, 2013; Huang et al,
360 2014a).

361 **5 Conclusions**

362 (1) The Eocene Sha-3 Member in the offshore Bohai Bay Basin experienced considerable post-depositional
363 modification that has resulted in a distinct change of its appearance. The present-day structural framework of this
364 set of strata reflects the combined result of multiple episodes of modification, among which, basin inversion
365 during the late Eocene was the most intense.

366 (2) The Bozhong area formed a large sedimentary depression during the deposition of the Sha-3 Member.
367 Many contemporaneous sags in this area, including the Qinnan, Shan'an, Huanghekou, Bodong and Miaoxi sags,
368 were connected to the major Bozhong sag. The main body of the Shijiutuo Rise, the western Bonan Low Rise
369 and the Bodong Low Rise did not exist at the time of accumulation of the Sha-3 Member.

370 (3) Following accumulation of the Sha-3 Member, NWW-trending faults exerted an important role in the
371 formation of the western sags, including the Shan'an and Chengbei sags. The process of subsidence of the large
372 Bozhong Depression during late Eocene was likely controlled by the interaction of the extension in a
373 NNE-SSW direction and deep geological process. The NNE-trending Tan-Lu Fault Zone did not exhibit obvious
374 control on the formation of the Miaoxi and Bodong sags. Following the early faulted evolution of the basin
375 during accumulation of the Paleogene Kongdian Formation, the Sha-3 and Sha-4 members record a regional
376 faulted-depression stage in the Bohai Bay Basin.

377 **Acknowledgements**

378 This study was supported by National Natural Science Foundation of China (Grant No. 41330315), National
379 Science and Technology Major Project (Grant No. 2011ZX05023001-002) and MOST Special Funds from the
380 State Key Laboratory of Continental Dynamics (Grant No. BJ081334). We are grateful to Wu Jingfu, Zhang
381 Gongcheng, Liang Jianshe, Wu Keqiang of CNOOC for their constructive comments. Graduate students Mao
382 Wei and Zhu Bin, and Ph.D. students Jia Nan, Dengyu of Northwest University contributed to the data collection
383 and the editing of maps; their assistance is greatly appreciated. We thank the reviewers and editors for their
384 helpful suggestions.

385 **References**

- 386 Allen, M. B., Macdonald, D. I. M., Zhao, X., Vincent, S. J. and Brouet-Menzies, C., 1997. Early Cenozoic two-phase
387 extension and late Cenozoic thermal subsidence and inversion of the Bohai Basin, northern China. *Marine and petroleum*
388 *Geology*, 14(7–8): 951–972.
- 389 Brandon, M.T., 1996. Probability density plots for fission-track grain age distributions. *Radiation Measurements*, (26):663–
390 676.
- 391 Deng Yunhua, 1999. The differentiation of hydrocarbon accumulation among sags and rises in Bohai bay basin. *China*
392 *Offshore Oil and Gas (Geology)*, 13(6):401–405 (in Chinese with English abstract).
- 393 Editorial Committee on Hydrocarbon Geology of Nearshore and Adjacent Areas (ECOHA), 1990. *Petroleum geology of*
394 *China* (Vol. 16, Grade 1). Beijing: Petroleum Industry Press, 83–85 (in Chinese).
- 395 Gong Zaisheng, 1997. *China offshore oil and gas fields*. Beijing: Petroleum Industry Press, 1–223 (in Chinese).
- 396 Han Shaojia, Zhao Junfeng, Liu Chiyang, Lu Jianjun and Jia Nan, 2014. Restoration of the original sedimentary extent of
397 Miaoxi Sag in Bohai Sea during the sedimentary period of the third member of Shahejie Formation in Paleogene.
398 *Geological Review*, 60(2):339–347 (in Chinese with English abstract).
- 399 Huang L, Liu C, Wang Y, Zhao, J., and Mountney, N. P., 2014b. Neogene–Quaternary postrift tectonic reactivation of the
400 Bohai Bay Basin, eastern China. *AAPG Bulletin*, 98(7):1377 – 1400.
- 401 Huang L., Liu C., 2014a. Evolutionary characteristics of the sags to the east of Tan–Lu Fault Zone, Bohai Bay Basin (China):
402 Implications for hydrocarbon exploration and regional tectonic evolution. *Journal of Asian Earth Sciences*, 79: 275–287.
- 403 Huang, L., Liu C, Kusky T, 2015. Cenozoic evolution of the Tan – Lu Fault Zone (East China)—Constraints from seismic
404 data. *Gondwana Research*, doi.org/10.1016/j.gr.2014.09.005
- 405 Huang Lei, Liu Chiyang, Zhou Xinhua and Wang Yingbin, 2012a. The important turning points during evolution of
406 Cenozoic basin offshore the Bohai Sea: evidence and regional dynamics analysis. *Science China: Earth Science*,
407 42(6):893–904.
- 408 Huang Lei, Wang Yingbin, 2012b. Characters and genesis of Bozhong ring structure belt and its oil geology significance.
409 *Chinese Journal of Geology*, 47(2):318–332 (in Chinese with English abstract).
- 410 James, D. L., 1995. Mechanics of basin inversion from worldwide examples. *Basin Inversion*, Geological
411 Society, London, Special Publication, (88):39–57.

412 Jarosinski, M., Beekman, F., Matenco, L. and Cloetingh, S., 2011. Mechanics of basin inversion: Finite element modeling
413 of the Pannonian Basin System. *Tectonophysics*, (502): 121 – 145.

414 Jiang Hua, Wang Hua, Lin Zhengliang, Fang Xinxin, Zhao Shue and Ren Guiyuan, 2009. Periodic rifting activity and its
415 controlling on sedimentary filling of Paleogene period in Nanpu sag. *Acta Sedimentologica Sinica*, 27(5):976–982 (in
416 Chinese with English abstract).

417 Kevin, C.H., Kathy, A.H., Gareth, T.C., Andrea, J. O., Pual B. O. and Richardson, M. J., 1995. Inversion around the Bass
418 basin, SE Australia. In: *Basin Inversion*, Geological Society, London, Special Publications, (88):525–547.

419 Lai Weicheng, Xu Changgui, Wang Xiaogang, Wang Cunzhi and Liu Fuping, 2007. Study on Paleogene Sequence
420 stratigraphy and sedimentary systems and a discussion on hydrocarbon exploration directions in Qinnan Sag. *China
421 Offshore Oil and Gas*, 19(5):300–304 (in Chinese with English abstract).

422 Li Desheng, 1997. Geological structure and hydrocarbon distribution in the Bohai Bay basin. In: Zhang Wenzhao eds. *Large
423 nonmarine oil fields in China*. Beijing: Petroleum Industry Press, 120–134 (in Chinese).

424 Li Jianping, Zhou Xinhuai and Lu Dingyou, 2011. Distribution and evolution of Paleogene delta systems in offshore Bohai
425 Bay basin. *China Offshore Oil and Gas*, 23(5):293–298 (in Chinese with English abstract).

426 Li Sanzhong, Zhao Guochun, Dai Liming, Zhou Lihong, Liu Xin, Suo Yanhui, M. Santosh. 2012b. Cenozoic faulting of the
427 Bohai Bay Basin and its bearings on the destruction of the eastern North China Craton. *Journal of Asian Earth Sciences*, 47:
428 80–93.

429 Li Sanzhong, Zhao Guochun, Dai Liming, Liu Xin, Zhou Lihong, M. Santosh, Suo Yanhui. 2012a. Mesozoic Basins in eastern
430 China and their Bearings on the deconstruction of the North China Craton. *Journal of Asian Earth Sciences*, 47: 64–79.

431 Liu Chiyang and Sun Haishan, 1999. Classification of reformed basin. *Xianjiang Petroleum Geology*, 20(2):79–83 (in
432 Chinese with English abstract).

433 Liu Chiyang and Yang Xingke, 2000. Thinking for researches and oil–gas assessment of reformed basins. *Oil and Gas
434 Geology*, 21(2):11–14 (in Chinese with English abstract).

435 Liu Guangxia, Zhang Xian, He Weimin, Shen Jingxiu and Tang Xifeng, 1996. Research on Curie geothermal surface in Bohai
436 Sea and its adjacent region. *Seismology and Geology*, 18(4):398–402 (in Chinese with English abstract).

437 Marco, B., Federico, S. and Benedetta, A., 2012. Basin inversion and contractional reactivation of inherited normal faults—A
438 review. *Tectonophysics*, (522–523): 55 – 88.

439 Mike S., 1999. Mechanics of basin inversion. *Tectonophysics*, (305):109–120.

440 Qi Jiafu, Deng Rongjing, Zhou Xinhuai and Zhang Kexin, 2008. The Tanlu fault belt in the Cenozoic offshore Bohai Bay
441 basin. *Science China (Series D): Earth Science*, 38(App.1): 19–29.

442 Sanzhong Li, Yanhui Suo, M. Santosh, Liming Dai, Shan Yu, Shujuan Zhao, Chong Jin. 2013. Mesozoic to Cenozoic
443 intracontinental dynamics of the North China Block. *Geological Journal*, 48(5): 543–560.

444 Song, T., 1997. Inversion styles in the Songliao basin (northeast China) and estimation of the degree of inversion.
445 *Tectonophysics*, (283):173–188.

446 Susanne, J.H. B., Adrian, O. Pfiffner and Beaumont, C., 2009. Inversion of extensional sedimentary basins: A numerical
447 evaluation of the localisation of shortening. *Earth and Planetary Science Letters*, 288:492–504.

448 Teng Jiwen, Zhang Zhongjie, Zhang Bingming, Yang Dinghui, Wan Zhichao and Zhang Hui, 1997. Geophysical fields and
449 background of exceptional structure for deep latent mantle plume in Bohai Sea. *Acta Geophysica Sinica*, 40(4):468–480 (in
450 Chinese with English abstract).

451 Turner, J.P. and Williams, G.A., 2004. Sedimentary basin inversion and intra–plate shortening. *Earth–Science Reviews*, (65):
452 277 – 304.

453 Wang Guochun, 1998. Relationship of Tanlu fault to the inversion and flower structures in Bohai Bay. *China Offshore Oil
454 and Gas (Geology)*, 12(5):289–295 (in Chinese with English abstract).

455 Wang Liangshu, Liu Shaowen, Xiao Wenying, Li Cheng, Li Hua, Guo Suiping, Liu Bo, Luo Yunhui and Cai Dongsheng,
456 2002. The heat flow distribution in the offshore Bohai Bay basin. *China Science Bulletin*, 47(2):151–155 (in Chinese with
457 English abstract).

458 Wu Lei, Xu Huaimin and Ji Hancheng, 2006. Evolution of sedimentary system and analysis of sedimentary source in
459 Paleogene of Bozhong sag, Bohai Bay. *Marine Geology & Quaternary Geology*, 26(1):81–88 (in Chinese with English
460 abstract).

461 Xia Qinglong, Zhou Xinhuai, Li Jianping, Xin Renchen and Xu Changgui, 2012. *Sequence, sedimentary evolution and
462 reservoir distribution of the Paleogene in the offshore Bohai Bay basin*. Beijing: Petroleum Industry Press, 1–178 (in
463 Chinese).

464 Xu Changgui, Yu Shui, Lin Chang Song, Wang Xin, Wang Yuechuan and Li Huiyong, 2008. Structural styles of the Paleogene
465 lacustrine basin margin and their control on sedimentary sequences in Bohai Sea area. *Journal of Palaeogeography*,
466 10(6):627–635 (in Chinese with English abstract).

467 Yang, Y. and Xu, T., 2004. Hydrocarbon habitat of the offshore Bohai Basin, China. *Marine and Petroleum Geology*,
468 (21):691–708.

469 Zhang Gongcheng, 2000. Tectonic framework and prolific hydrocarbon depressions in Bohai Bay. *China Offshore Oil and Gas
470 (Geology)*, 14(2):93–99 (in Chinese with English abstract).

471 Zhao Chenglin, Yang Congxiao and Liu Menghui, 1996. *The Paleogene lithofacies and paleogeography of the offshore Bohai
472 Bay basin*. Beijing: Petroleum Industry Press, 1–168 (in Chinese).

473 Zhao Junfeng, Liu Chiyang, Liang Jiwei, Wang Xiaomei, Yu Lin, Huang Lei and Liu Yongtao, 2010. Restoration of the
474 original sedimentary boundary of the middle Jurassic Zhiluo Formation–Anding Formation in the Ordos basin. *Acta*

- 475 *Geologica Sinica*, 84(4):553–569 (in Chinese with English abstract).
- 476 Zhou Donghong, Pang Xiaojun, Wang Guanmin and Zhang Xuefang, 2011. The controlling of Paleogene fault activity on
477 sandbody distribution in Bozhong depression– taking Shinan fault zone for example. *Journal of Oil and Gas Technology*,
478 33(11):14–18 (in Chinese with English abstract).
- 479 Zhou Lihong, Fu Lixin, Lou Da, Lu Yi, Feng Jiangquan, Zhou Shuhui, M. Santosh, Sanzhong Li. 2012. Structural anatomy
480 and dynamics of evolution of the Qikou Sag, Bohai Bay Basin, China. *Journal of Asian Earth Sciences*,47: 94–106.
- 481 Zhu Weilin, Mi Lijun and Gong Zaisheng, 2009. *Hydrocarbon accumulation and exploration in offshore Bohai Bay basin*.
482 Beijing: Science Press, 1–326 (in Chinese).
- 483 Zhu Weilin, Mi Lijun, Gao Yangdong, Gao Le and Zhong Kai, 2013. The discovery of giant and major fields has given
484 impetus to reaching a new peak in hydrocarbon exploration offshore China: a review of 2012.offshore exploration in China.
485 *China Offshore Oil and Gas (Geology)*, 25(1):6–12 (in Chinese with English abstract).
- 486 Ziegler, P.A., Cloetingh, S. and Wees, J.D., 1995. Dynamics of intra–plate compressional deformation: the alpine foreland
487 and other examples. *Tectonophysics*, (252): 7–59.
- 488

489 **About the first author**

490 **Zhao Junfeng.** Born in 1975, Zhao received his Ph.D. degree from Northwest University, China, in 2007. He is
491 currently Associate Professor of Geology at Northwest University. His research interests are sedimentology and
492 basin analysis.

493

494

495 Table 1. Generalized division of the stratigraphy and the basin evolution stages of the Bozhong Depression, offshore Bohai
 496 Bay Basin. Modified after Zhu et al. (2009).

Lithostratigraphy division					Bottom age (Ma)	Seismic interface	Tectonic stages	
System	Series	Formation	Member	Code				
Quaternary		Pingyuan			Qp	2.6	Post-rift thermal subsidence	
Neogene	Pliocene	Minghuazhen	Upper	N ₁ m ⁺	5.3	T ₀		
			Lower	N ₁ m ¹	12.0			
	Miocene		Guantao	Upper	N ₁ g ⁺			T ₁
				Lower	N ₁ g ¹	24.6		T ₂
Paleogene	Oligocene	Dongying	Dong-1	E ₃ d ¹	27.4	T ₃		
			Dong-2	E ₃ d ²	30.3			
			Dong-3	E ₃ d ³	32.8			
	Eocene	Shahejie	Sha-1	E ₃ s ¹	36.0	T ₄		
			Sha-2	E ₃ s ²	38.0	T ₅		
			Sha-3	E ₃ s ³	42.0	T ₆		
			Sha-4	E ₃ s ⁴	50.5	T ₇		
	Paleocene	Kongdian	Kong-1	E ₂ k ¹		T ₈		
			Kong-2	E ₂ k ²				
			Kong-3	E ₂ k ³	65.0			
Pre-Paleogene								

497
 498 Table 2. Classification of types of inversion of the Sha-3 Member in the Bozhong Depression, offshore Bohai Bay Basin.

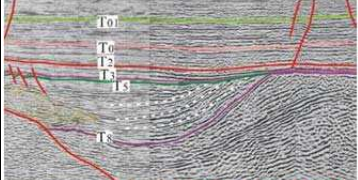
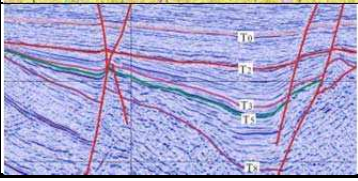
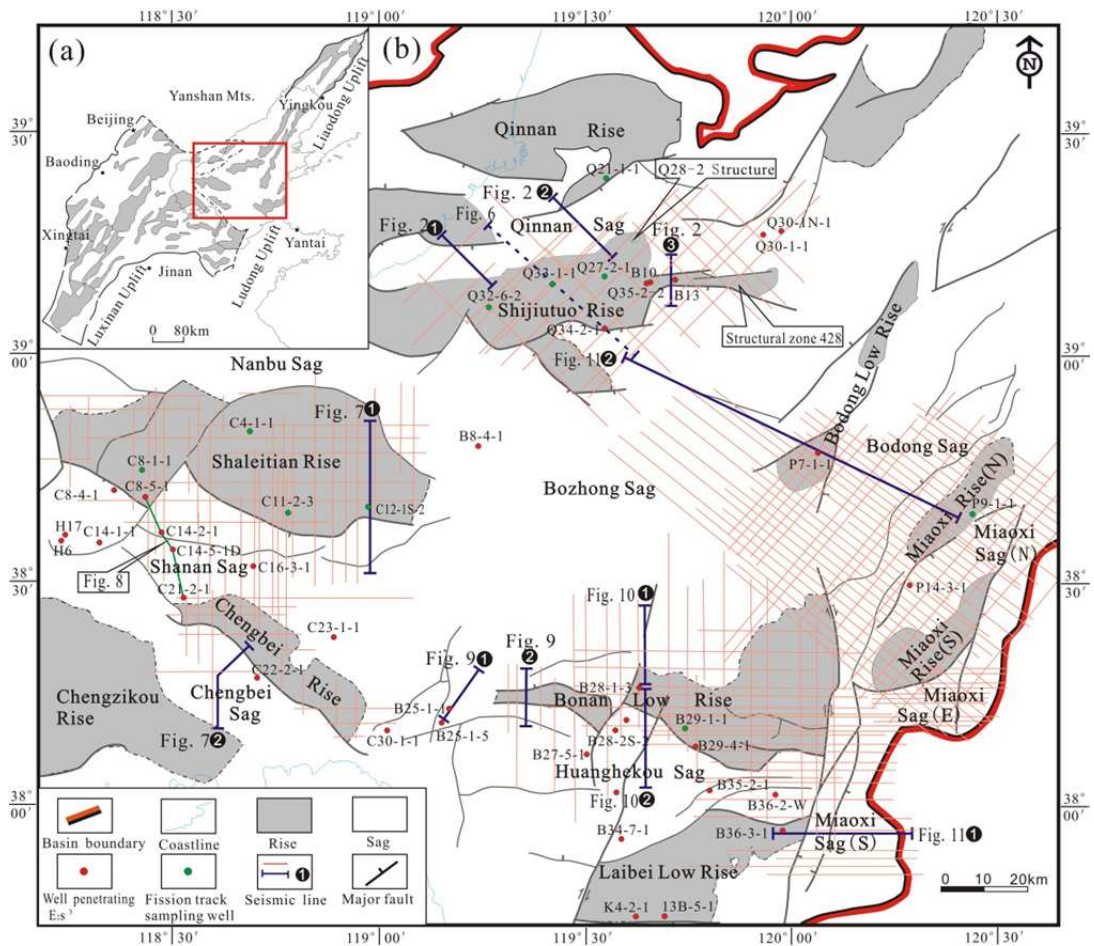
Type	Strata contact relationship	Typical profiles	Modification intensity	Results	Representative cases
Tilting by compression	Overlying and underlying strata of T ₅ interface is unconformable		High intensity	The Sha-3 member eroded partly and separated by post forming rise	Southern Qinnan sag, middle-southern Miaoxi sag
Lifting by block faulting	T ₅ and T ₃ interfaces merged together and conformable with T ₈ interface		Moderate intensity	Forming mall scale bulges and sub-sags in the same original sag	Bozhong-Bodong sags, Liaoxi sag, western Shan'an sag
Tilting by compressional strike-slip	Overlying and underlying strata of T ₅ interface is unconformable with steep contact angle		Low intensity	The Sha-3 member looks continuous, only eroded at the high part, forming distinct strata occurrence	Liaodong high-Liaodong sag
Regional uplifting	Overlying and underlying strata of T ₅ interface mainly is conformable, only unconformable at the marginal area		Weak	The Sha-3 member looks continuous, just eroded at the margin	Chengbei sag, Shan'an sag, etc.

Table 3. Data and results of fission-track analysis of apatite samples from the Bozhong area.

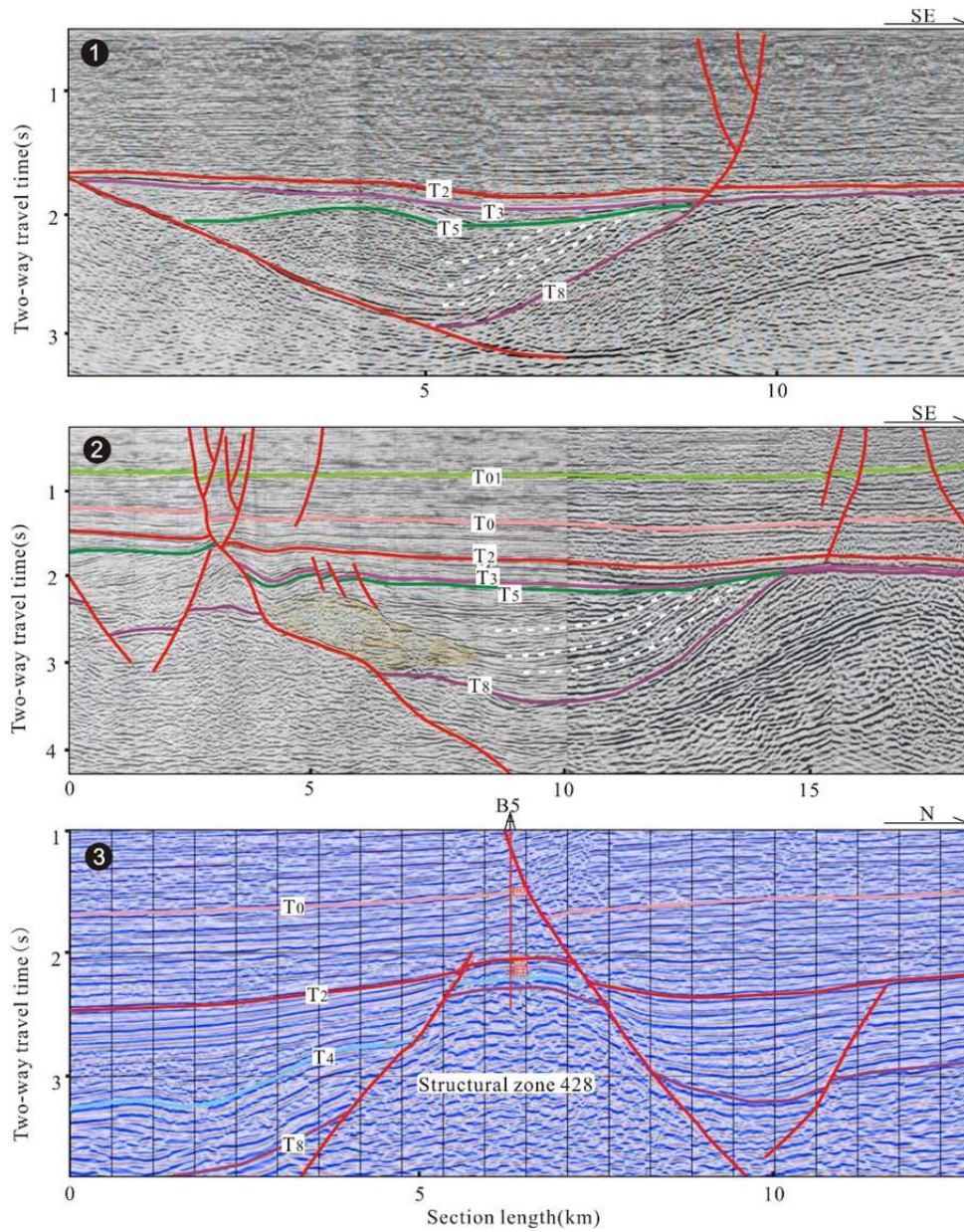
Sampling well	Lithology	Strata	<i>n</i>	ρ_s ($10^5/cm^2$) (Ns)	ρ_i ($10^5/cm^2$) (Ni)	ρ_d ($10^5/cm^2$) (N)	$P(\chi^2)$ (%)	Central age (Ma) ($\pm 1\sigma$)	Pooled Age (Ma) ($\pm 1\sigma$)	<i>L</i> (μm) (N)
Q21-2-1	Granite	Pre-Sinian	25	5.862 (2808)	41.103 (19689)	13.282 (9117)	0	34 \pm 2	33 \pm 2	12.7 \pm 1.5 (104)
Q27-2-1	Clastic rock	Mesozoic	30	1.094 (274)	5.985 (1499)	12.926 (9117)	32.5	42 \pm 4	42 \pm 4	12.2 \pm 1.5 (33)
Q32-6-2	Andesite	Mesozoic	28	3.862 (1408)	23.596 (8603)	12.66 (9117)	0	38 \pm 3	37 \pm 2	11.7 \pm 1.4 (103)
Q33-1-1	Andesite	Mesozoic	30	0.388 (199)	1.618 (829)	12.66 (9117)	48.5	53 \pm 5	53 \pm 5	12.4 \pm 1.5 (101)
C8-1-1	Granite	Pre-Cambrian	28	1.419 (1003)	10.975 (7756)	12.66 (9117)	0.1	28 \pm 2	29 \pm 2	12.3 \pm 1.4 (101)
C4-1-1	Granite	Proterozoic	15	0.539 (53)	15.148 (1489)	12.66 (9117)	0	10.3 \pm 2.6	7.9 \pm 1.2	
C11-2-3	Calclutite	Archean	31	3.033 (560)	11.321 (2090)	12.926 (9117)	0	58 \pm 6	61 \pm 4	12.3 \pm 1.5 (100)
C12-1S-2	Granite	Proterozoic	30	2.657 (1473)	20.552 (11394)	13.282 (9117)	0	31 \pm 2	30 \pm 2	11.8 \pm 1.5 (103)
B29-1-1	Clastic rock	Mesozoic	29	0.695 (227)	7.581 (2563)	13.628 (9117)	78.7	21 \pm 2	21 \pm 2	11.1 \pm 2.1 (69)
P9-1-1	Volcanic rock	Proterozoic	30	0.861 (331)	5.743 (2208)	13.993 (9117)	99.3	37 \pm 3	37 \pm 3	11.8 \pm 1.7 (75)

Notes: ρ_s , ρ_i , and ρ_d are spontaneous track density, induced track density (track number over area), and standard track density respectively; N_s , N_i , and N_d are numbers of spontaneous track, induced track, and standard track respectively; *L* is mean track length ($\pm\sigma$); $P(\chi^2)$ is χ^2 test value.

501
502
503

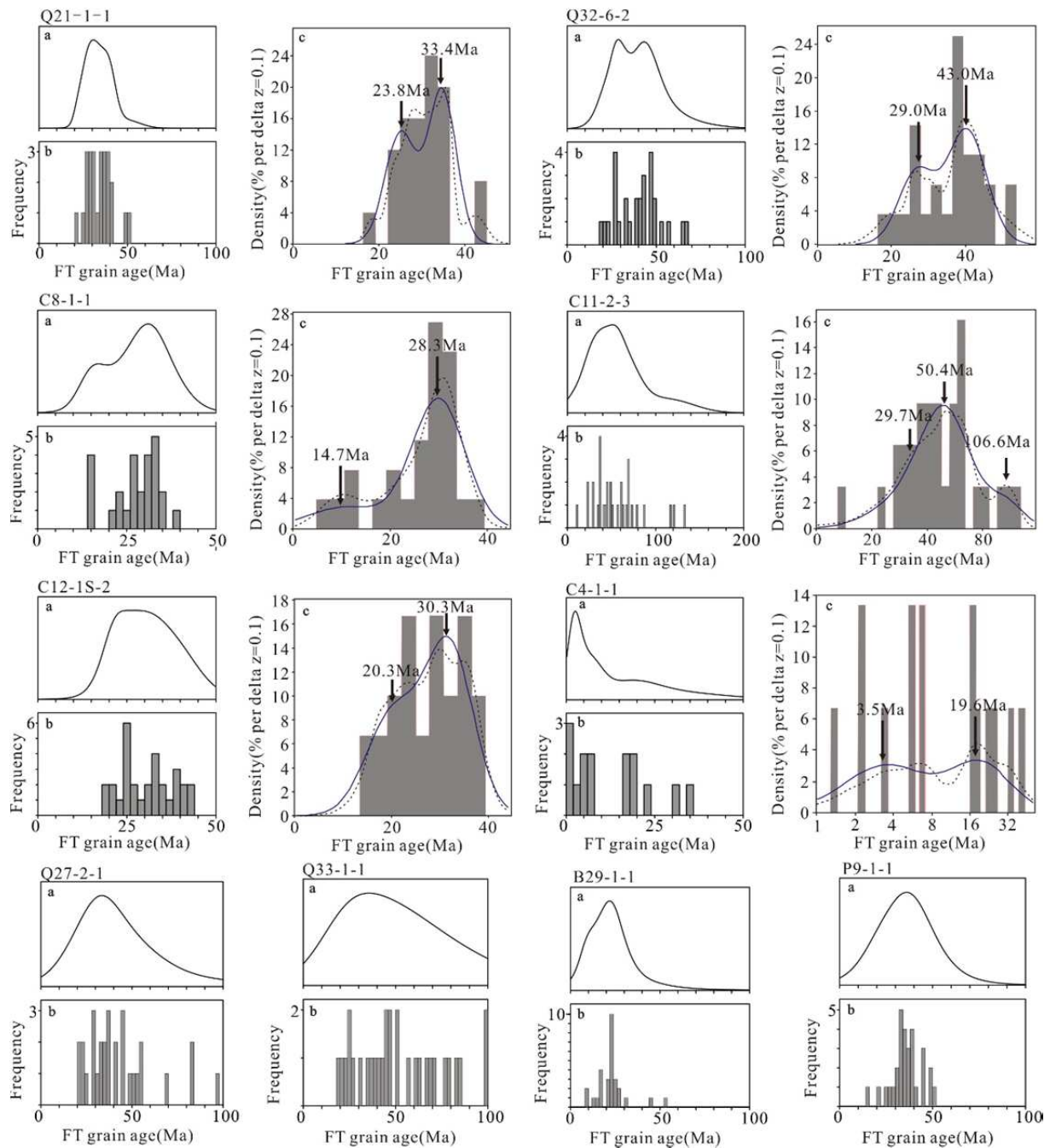


504
505
506
Figure 1. (a) Regional location of the Bozhong Depression in the Bohai Bay Basin. (b) Geological framework of the Bozhong Depression. The location of seismic profiles and wells used in this study are indicated.



507
 508
 509

Figure 2 Representative seismic profiles across the north-western part of the Bozhong Depression (see Fig. 1 for location).



510

511

512

513

Figure 3. Distribution of single apatite grain ages; 10 samples in total. (a) Gaussian fitting curves; (b) histogram of single apatite grain ages; (c) least-square fitting curves.

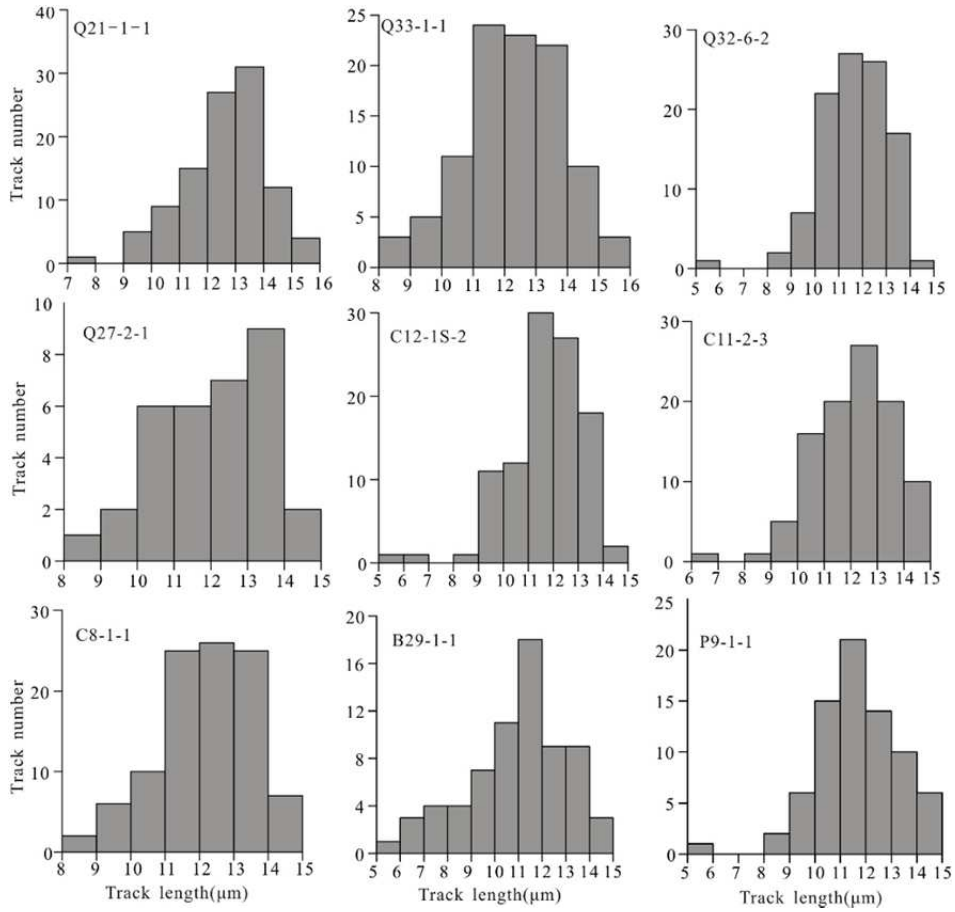
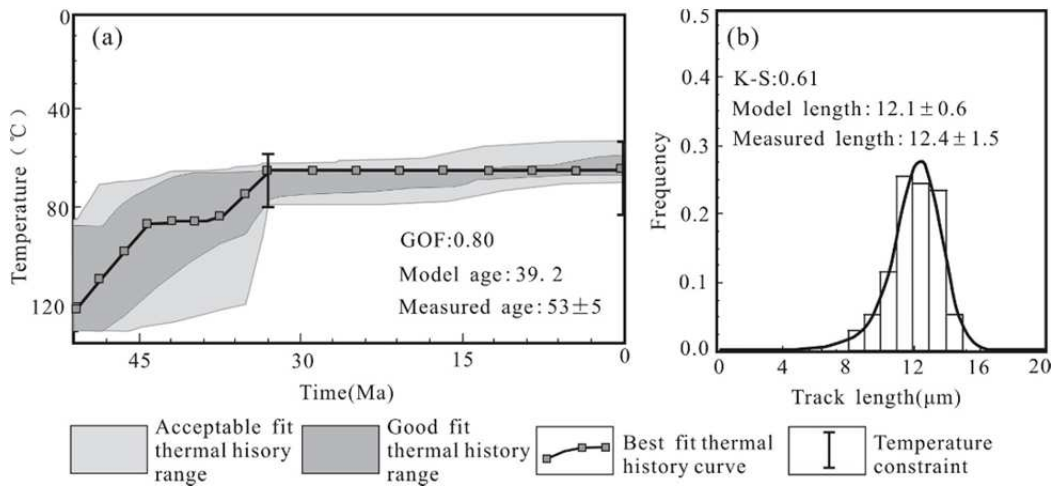


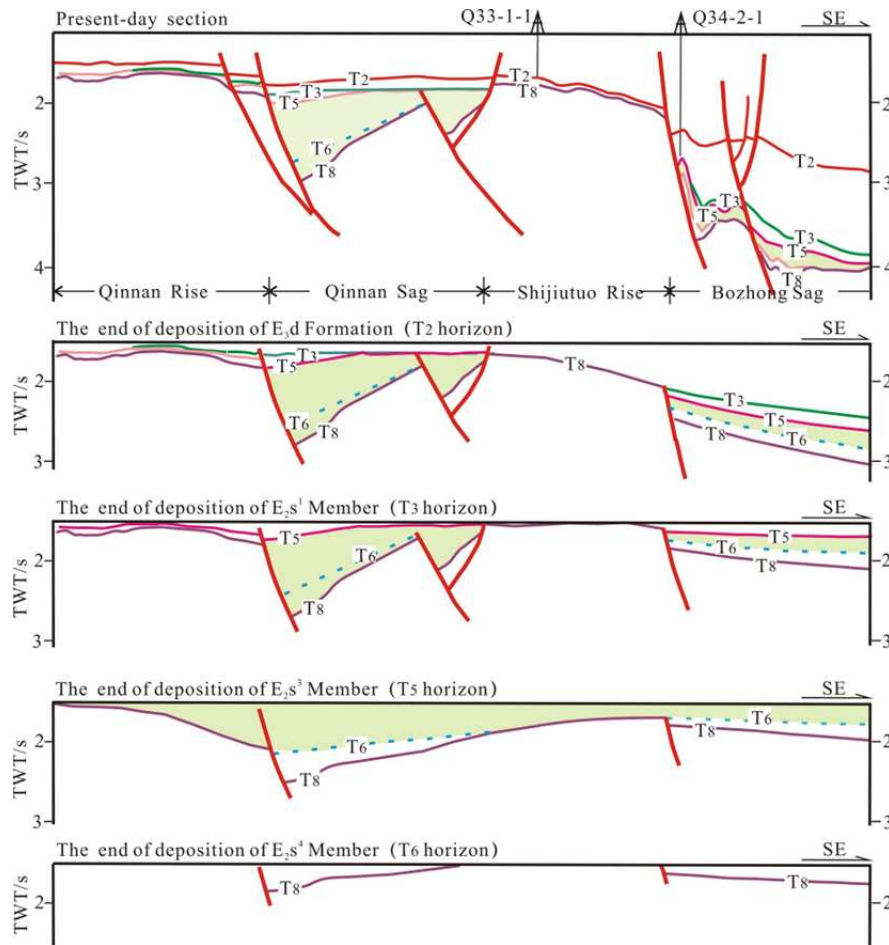
Figure 4. Histograms of the fission-track length distributions.

514
515
516
517



518
519
520

Figure 5. Apatite fission-track (AFT) modeling of sample Q33-1-1. (a). The modeling thermal history route; (b) Histogram showing the comparison between the measured and modeled track-length distributions.



521
 522 Figure 6. Profiles showing the geological evolution of the Qinnan Sag, Shijiutuo Rise and Bozhong Sag, northwestern
 523 Bozhong Depression (see Fig. 1 for location).
 524

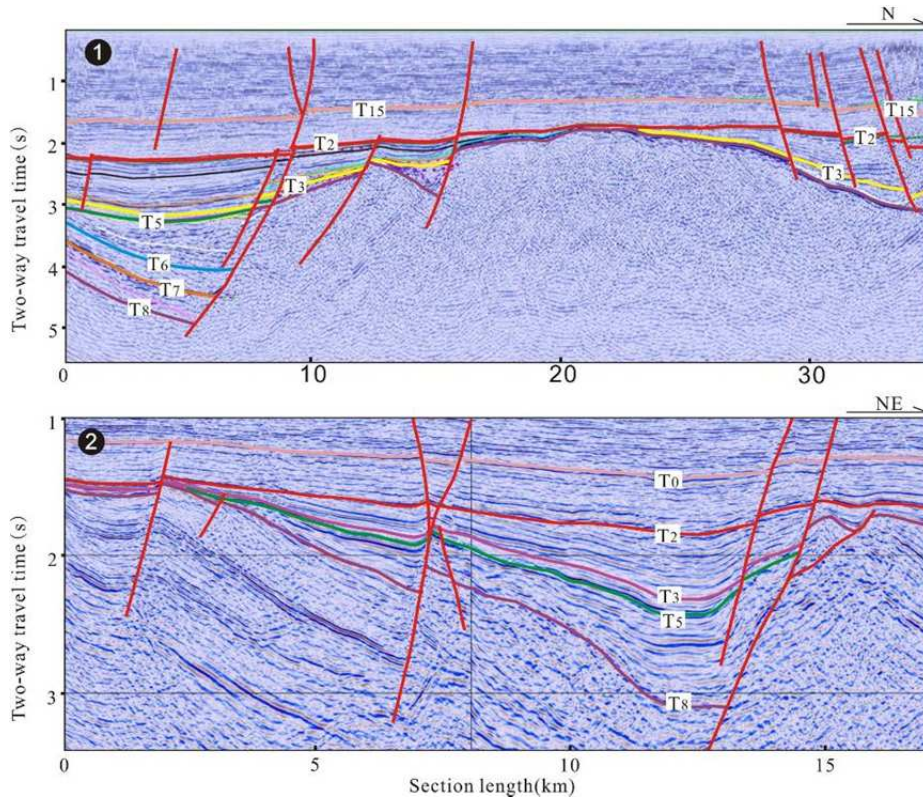


Figure 7. Representative seismic profiles across the western part of the Bozhong Depression (see Fig. 1 for location).

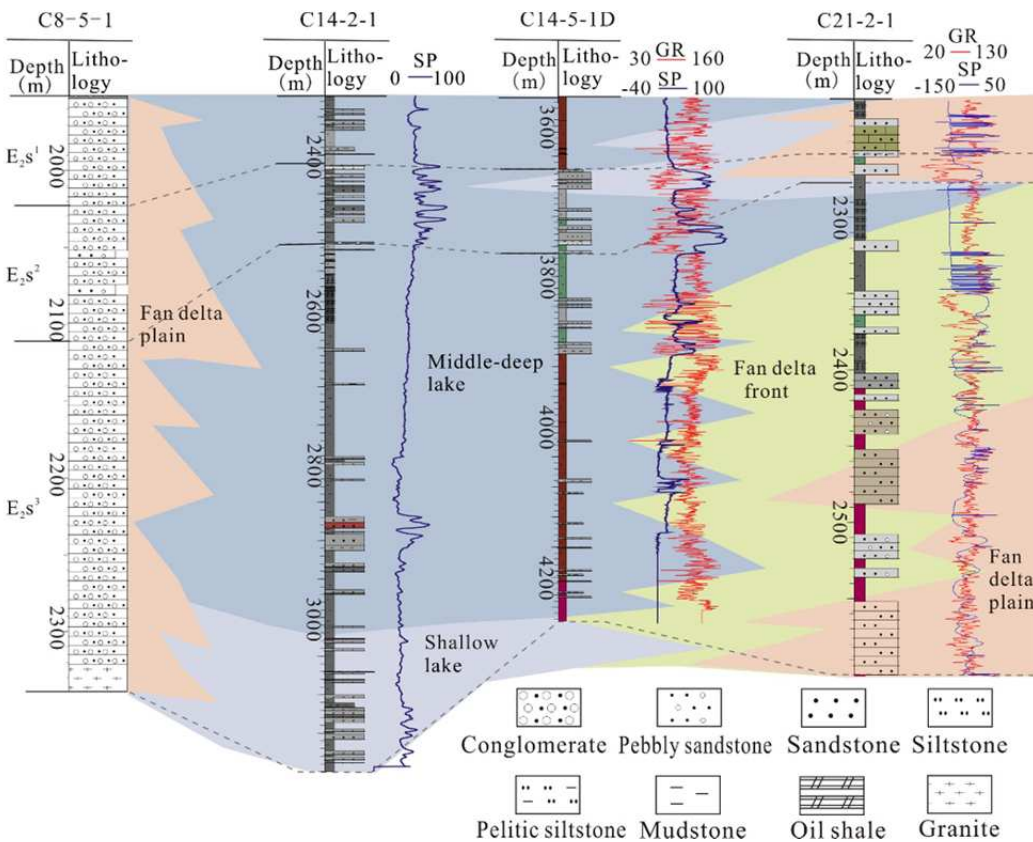


Figure 8. Cross section and summary well-logs depicting the sedimentary facies arrangement for the Sha-3 Member, Shanan Sag (see Fig. 1 for location of wells).

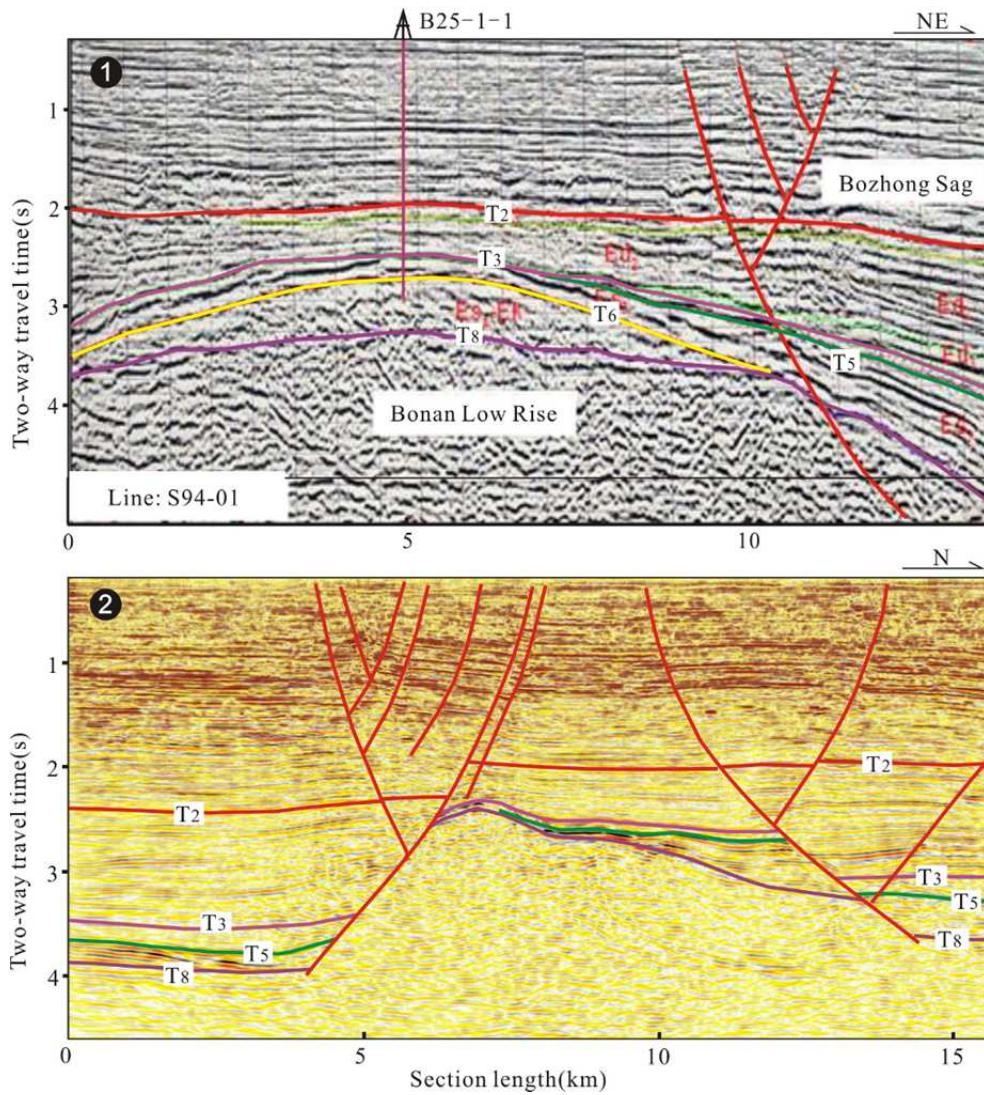
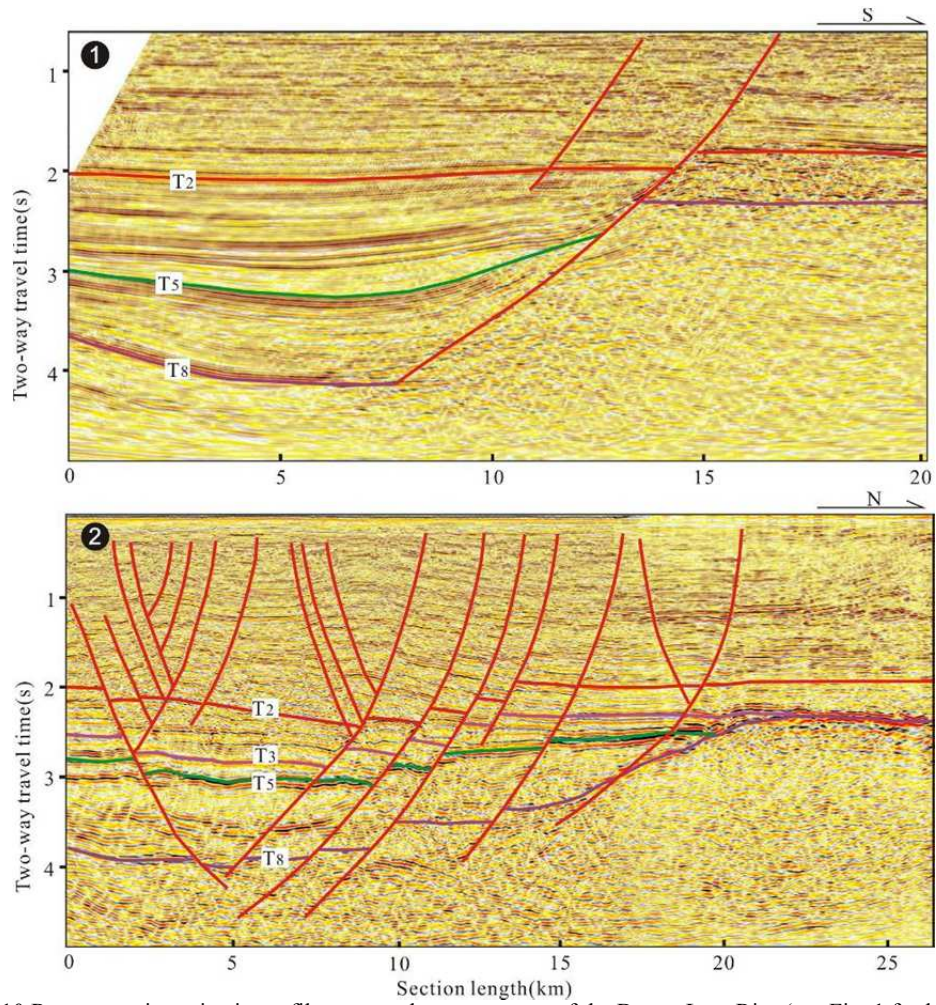


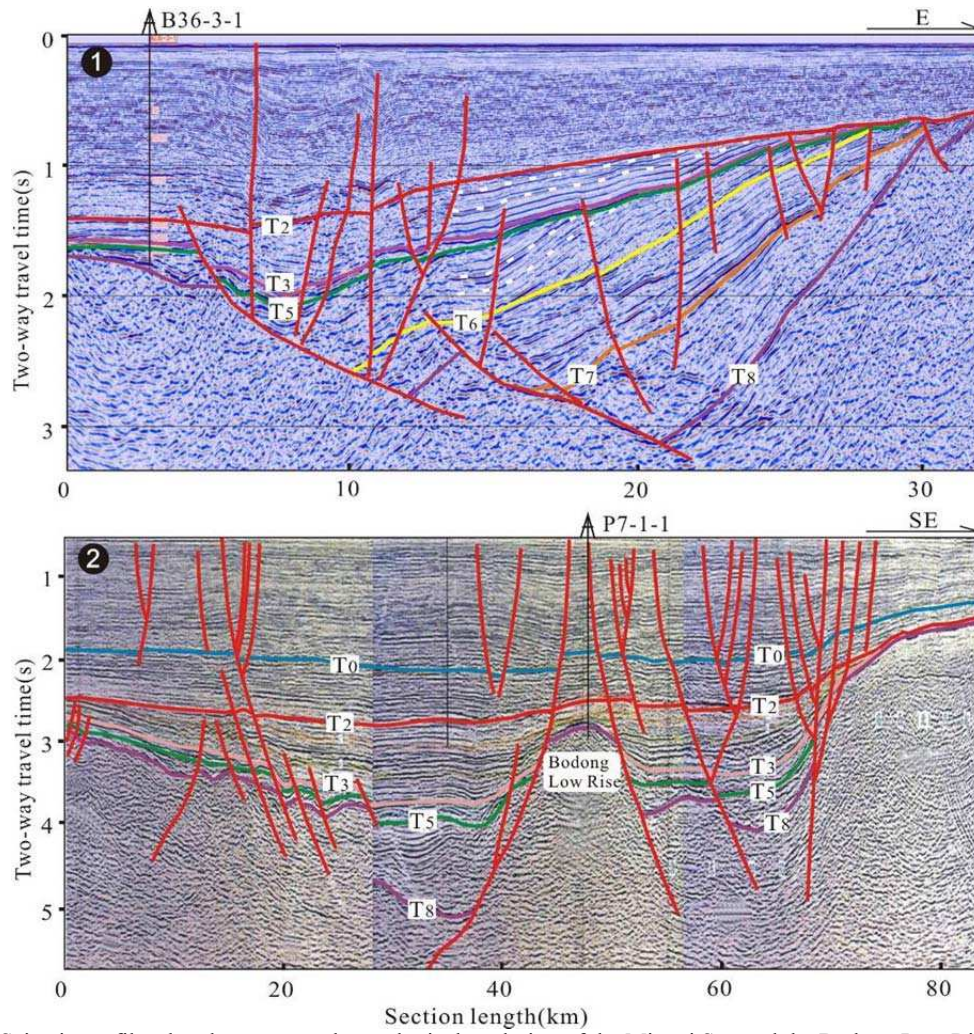
Figure 9. Representative seismic profiles across the western part of the Bonan Low Rise (see Fig. 1 for location).

532
533
534



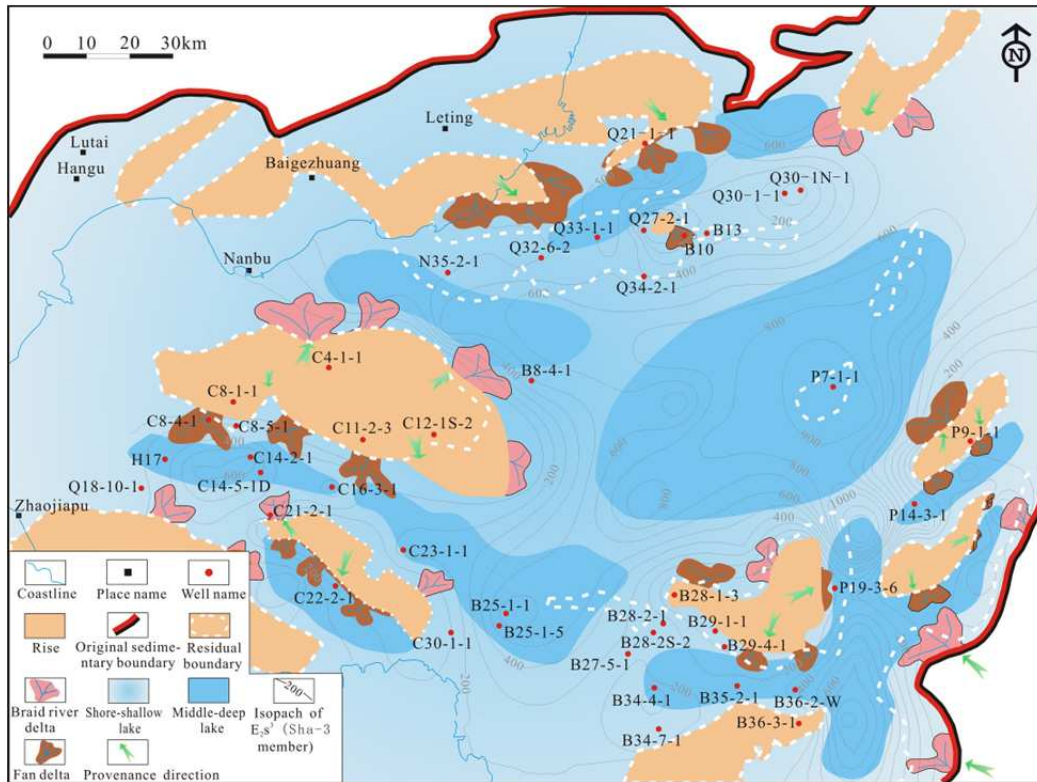
535
536

Figure 10 Representative seismic profiles across the eastern part of the Bonan Low Rise (see Fig. 1 for location).



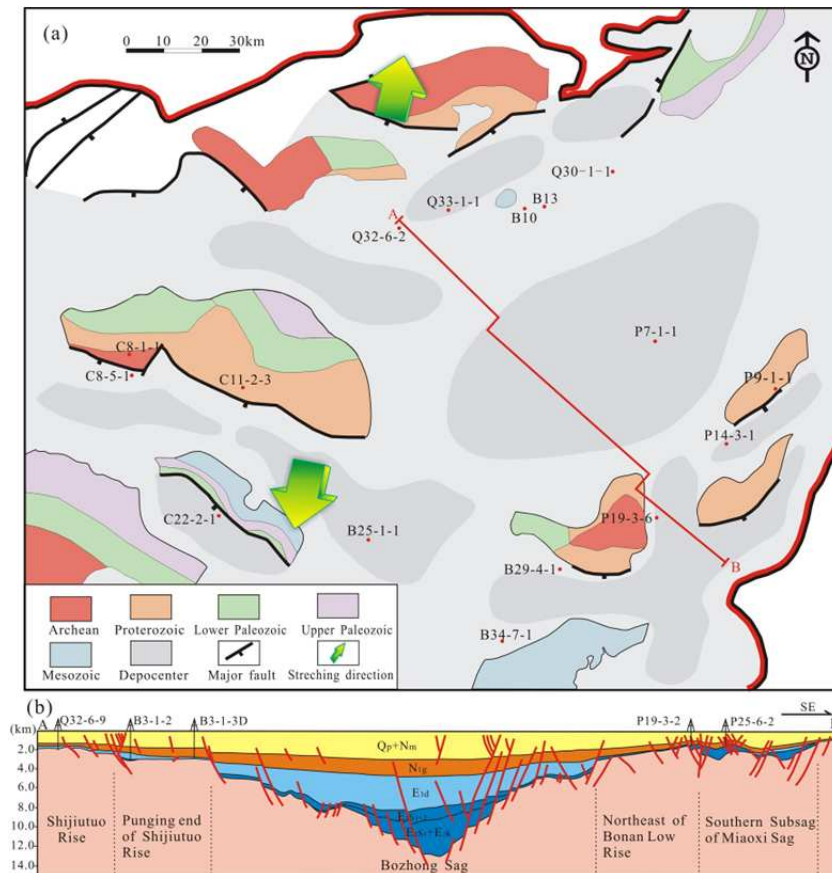
537
 538
 539
 540

Figure 11. Seismic profiles that demonstrate the geological evolution of the Miaoxi Sag and the Bodong Low Rise (see Fig. 1 for location).



541
542

Figure 12 Original sedimentary extent of the Eocene Sha-3 Member in the Bozhong Depression, offshore Bohai Bay basin.



543
544
545
546
547

Figure 13. Depositional setting of the Eocene Sha-3 Member in the Bozhong Depression. (a) Plan-view map showing the paleogeography, distribution of basement rocks associated with rises and major faults. Distribution of basement rocks is modified after Deng et al.(2008). (b) Regional cross section showing the present-day architectural configuration of the Bozhong Depression and its style of Cenozoic infill.